

PSI-PR-97-11  
FTUV/97-13  
IFIC/97-13  
March 1997

# Discovering and Studying Bileptons with $e^-e^-$ Collisions

Frank Cuypers

cuyers@psi.ch

*Paul Scherrer Institute, CH-5232 Villigen PSI, Switzerland*

Martti Raidal

raidal@titan.ific.uv.es

*Department of Theoretical Physics and IFIC,  
University of Valencia, 46100 Burjassot, Valencia, Spain*

---

## Abstract

We analyze the prospects for discovering and unraveling the nature of doubly-charged bileptons at a linear collider of the next generation running in its  $e^-e^-$  mode. We stress the importance of initial state radiation, beam spread and polarization, and compute the discovery bounds. The gauge nature of vector bileptons can be determined by studying hard photon emission.

*Keywords:* bileptons, dileptons, new physics, new bosons,  $e^-e^-$  collisions

*PACS:* 14.80.-j, 12.60.-i, 12.10.Dm, 29.17.+w

---

## 1 Introduction

While the LHC offers an entry into the the high energy regime of the standard model with a significant opportunity for discovering new phenomena, a linear electron collider of the next generation [1] will provide a complementary program of experiments with unique opportunities for both discoveries and precision measurements. A major asset to fulfill this purpose is the versatility of linear colliders, as they can be operated in the four  $e^+e^-$ ,  $e^-e^-$ ,  $e^-\gamma$  and  $\gamma\gamma$  modes, with highly polarized electron and photon beams. Moreover, starting from a centre of mass energy of several hundred GeV, it will later be possible to upgrade these machines into the TeV range.

The  $e^-e^-$  running mode [2] is a particularly interesting feature of a high energy linear collider. One of the many promising processes which can be studied in this mode is the resonant production of doubly-charged bileptons. These particles are predicted by many extensions of the standard model, such as grand unified theories [3], theories with enlarged Higgs sectors [4], technicolour theories [5], theories of compositeness [6] and theories which generate neutrino majorana masses [7]. They may appear as scalars, vectors or Yang-Mills fields and can be classified in a model-independent way [8] much like leptoquarks [9].

The prospects for discovering doubly-charged bileptons through their  $s$ -channel resonance in  $e^-e^-$  collisions have been considered previously within the framework of specific models [10,11]<sup>1</sup>. We analyze these reactions here in more details taking into account properties of the beams and effects of initial state radiation. We also study in a model-independent way the range of bilepton couplings and masses which can be probed in the  $e^-e^-$  linear collider mode and we present ways of disentangling the different types of bileptons from each other.

For this we present in the following section the most general classification of bileptons together with their interaction lagrangians with fermions and gauge fields. In Section 3 we study the discovery potential of bileptons and we demonstrate that the radiative return to resonance due to initial state radiation may enable the discovery of bileptons without having to resort to a painstaking scan of centre of mass energies. In Section 4 we investigate how to distinguish between scalar and vector bileptons, and to which extent a determination of the gauge nature of vector bileptons is possible. We conclude in Section 6.

---

<sup>1</sup> We do not agree with the cross sections (3.30) and (1) stated in the first two references of Ref. [10], respectively.

## 2 Bilepton Classification

We define bileptons to be bosons which couple to two leptons and which carry two units of lepton number. Their interactions need not necessarily conserve lepton flavour, but otherwise we demand the symmetries of the standard model to be respected. The most general renormalisable lagrangian of this kind is of dimension four and involves seven bilepton fields  $L_1^+$ ,  $\tilde{L}_1^{++}$ ,  $L_{2\mu}^+$ ,  $L_{2\mu}^{++}$ ,  $L_3^0$ ,  $L_3^+$  and  $L_3^{++}$ . It is given by [8]

$$\begin{aligned}
\mathcal{L} = & -\lambda_1^{ij} L_1^+ \left( \bar{\ell}_i^c P_L \nu_j - \bar{\ell}_j^c P_L \nu_i \right) \\
& + \tilde{\lambda}_1^{ij} \tilde{L}_1^{++} \bar{\ell}_i^c P_R \ell_j \\
& + \lambda_2^{ij} L_{2\mu}^+ \bar{\nu}_i^c \gamma^\mu P_R \ell_j \\
& + \lambda_2^{ij} L_{2\mu}^{++} \bar{\ell}_i^c \gamma^\mu P_R \ell_j \\
& + \sqrt{2} \lambda_3^{ij} L_3^0 \bar{\nu}_i^c P_L \nu_j \\
& - \lambda_3^{ij} L_3^+ \left( \bar{\ell}_i^c P_L \nu_j + \bar{\ell}_j^c P_L \nu_i \right) \\
& - \sqrt{2} \lambda_3^{ij} L_3^{++} \bar{\ell}_i^c P_L \ell_j \\
& + \text{h.c.} \ ,
\end{aligned} \tag{1}$$

where the subscripts 1–3 label the dimension of the  $SU(2)_L$  representation to which the bileptons belong and the indices  $i, j = e, \mu, \tau$  stand for the lepton flavours. The chirality projection operators are defined as  $P_{R,L} = (1 \pm \gamma_5)/2$ .

In the following we shall concentrate on the doubly-charged members of the scalar singlet  $\tilde{L}_1^{--}$ , the vector doublet  $L_{2\mu}^{--}$  and the scalar triplet  $L_3^{--}$ . The coupling matrices of the two types of scalars to different flavours of leptons  $\lambda^{ij}$  are hermitian, while the coupling matrices for vectors are arbitrary. If  $CPT$  symmetry is imposed, the latter are either hermitian or anti-hermitian.

For the sake of definiteness we shall focus from now on the universal diagonal coupling matrix

$$\lambda^{ij} \equiv \lambda \begin{pmatrix} 1 & & \\ & 1 & \\ & & 1 \end{pmatrix} \ , \tag{2}$$

which would be a natural possibility for gauge bileptons. It is straightforward to implement a different choice, which we will do at the end of this section. Within the framework of the coupling matrix (2), though, the negative results of muonium-antimuonium conversion searches [12] imply approximately the same upper limit for the three doubly-charged bileptons on the ratio  $\lambda/m_B$ ,

where  $m_B$  is the bilepton mass:

$$\lambda \lesssim 0.5 m_B/\text{TeV} . \quad (3)$$

Up to now we have made no difference between ordinary vectors and Yang-Mills fields for the doublet  $L_{2\mu}$  bileptons. This distinction arises, however, when the interactions with the gauge fields are considered. In particular, the vector bilepton coupling to photon is described by the following lagrangian:

$$\begin{aligned} \mathcal{L} = & -1/2 (D_\mu L_{2\nu} - D_\nu L_{2\mu})^\dagger (D_\mu L_{2\nu} - D_\nu L_{2\mu}) \\ & - i \kappa eQ L_\mu^\dagger L_{2\nu} (\partial_\mu A_\nu - \partial_\nu A_\mu) , \end{aligned} \quad (4)$$

where the covariant derivative is given by

$$D_\mu = \partial_\mu - ieQA_\mu , \quad (5)$$

and  $Q$  is the charge of the bilepton, *i.e.*,  $Q = 2$  for our purposes. If the vector bileptons are Yang-Mills fields, the parameter  $\kappa$  in the second line of Eq. (4) takes the value one at tree level. On the other hand, for non-gauge vectors one expects a *minimal coupling* to the photon which is obtained when  $\kappa$  vanishes.

### 3 Discovering Bileptons

Muons can be pair-produced in  $e^-e^-$  collisions via the  $s$ -channel exchange of a doubly-charged scalar or vector bilepton, as depicted in Fig. 1. The differential cross sections of these reactions are given by

$$\frac{d\sigma(\tilde{L}_1^{--})}{dt} = \underbrace{\frac{(1+P_1)(1+P_2)}{4}}_{[RR]} \frac{\lambda^4}{2\pi} \frac{1}{(s-m_B^2)^2 + m_B^2\Gamma_B^2} , \quad (6)$$

$$\frac{d\sigma(L_{2\mu}^{--})}{dt} = \underbrace{\frac{1-P_1P_2}{2}}_{[LR]} \frac{\lambda^4}{8\pi s^2} \frac{t^2 + u^2}{(s-m_B^2)^2 + m_B^2\Gamma_B^2} , \quad (7)$$

$$\frac{d\sigma(L_3^{--})}{dt} = \underbrace{\frac{(1-P_1)(1-P_2)}{4}}_{[LL]} \frac{2\lambda^4}{\pi} \frac{1}{(s-m_B^2)^2 + m_B^2\Gamma_B^2} , \quad (8)$$

where  $P_1$  and  $P_2$  are the polarizations of the incoming electron beams,  $m_B$  and  $\Gamma_B$  are respectively the mass and width of the bilepton, and  $\lambda$  is the universal diagonal coupling (2). With this assumption on the structure of the leptonic couplings, the leptonic widths of the bileptons are given by [10,13]<sup>2</sup>

$$\Gamma_B = G \frac{\lambda^2}{8\pi} m_B, \quad \begin{cases} \tilde{L}_1 : G = 3, \\ L_{2\mu} : G = 1, \\ L_3 : G = 6. \end{cases} \quad (9)$$

Taking into account the current limits (3) on the possible values of the coupling  $\lambda$ , we see that bileptons as light as 200 GeV are bound to have a decay width which is significantly less than 1 GeV.

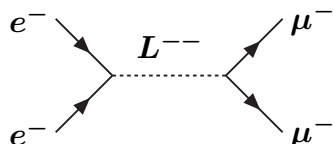


Fig. 1. Lowest order Feynman diagram inducing the process  $e^-e^- \rightarrow \mu^-\mu^-$ . The exchanged doubly-charged bilepton  $L^{--}$  can be one of the scalars  $\tilde{L}_1^-, L_3^-$  or the vector  $L_{2\mu}^-$ .

In the case of the doublet and triplet bileptons, the different members of the multiplet need not necessarily have the same mass. If the doubly-charged members of the multiplets turn out to be heavier than the singly-charged ones, the non-leptonic decay mode  $L^{--} \rightarrow L^-W^-$  can possibly also contribute to the total width [11]. However, only heavier bileptons can realistically accommodate a mass splitting exceeding the mass of the  $W$  boson. We therefore ignore this possibility here and assume purely leptonic decays of the bileptons.

Upon integrating Eqs (6–8) the total cross sections are

$$\sigma = S \frac{\lambda^4}{12\pi} \frac{s}{(s - m_B^2)^2 + m_B^2 \Gamma_B^2}, \quad \begin{cases} \tilde{L}_1 : S = 6 [RR], \\ L_{2\mu} : S = 1 [LR], \\ L_3 : S = 24 [LL]. \end{cases} \quad (10)$$

If the decay width of the bilepton is significantly larger than the beam spread, it is a good approximation to assume monochromatic electron beams. In this

<sup>2</sup> We do not agree with the width stated in the text of the second reference of Ref. [10].

case, the centre of the resonance can be precisely met, and the replacement  $s = m_B^2$  into Eq. (10) yields the cross section

$$\sigma = \frac{S}{G} \frac{16\pi}{3m_B^2} . \quad (11)$$

This cross section does not depend on the coupling to leptons, since any decrease/increase of the strength of the interactions also results into a decrease/increase of the decay width. In the observed cross section both effects result in a cancellation. Obviously, this result stops making sense for infinitesimal values of the coupling. Indeed, when the decay width is smaller than the beam spread, the latter needs to be taken in account [11]. If we approximate it by a box<sup>3</sup> of width  $R$  centered around the resonance, the observed cross section results from the convolution

$$\sigma = \int_{m_B-R/2}^{m_B+R/2} d\sqrt{s} \frac{1}{R} \sigma(\sqrt{s}) \simeq \frac{S}{G} \frac{\pi\lambda^2}{3m_B R} \quad (\Gamma_B \ll R \ll m_B) , \quad (12)$$

where a typical value for the beam spread is [14]

$$R = 10^{-2} \sqrt{s} . \quad (13)$$

Note that at a muon collider the corresponding spread would be of the order of  $4 \cdot 10^{-4} \sqrt{s}$  [15]. From this fact alone, plus the luminosity enhancement at nominal energy associated with the much reduced Brems- and beamstrahlung rates of colliding muon beams, results the possibility of generating hundred times more doubly-charged bileptons at a  $\mu^+\mu^-$  facility.

It may be that the resonance is so narrow that no significant tail extends on either side of the resonance. If this is the case and if the centre of mass energy were strictly confined within  $\sqrt{s} \pm R$ , it would be a long unpleasant task to find this resonance in the first place, through a minute energy scan. However, in practice initial state radiation and beamstrahlung will unavoidably perform a scan at lower energies. To obtain a rough idea of the effect, we approximate the centre of mass energy spectrum after initial state radiation to be of the form

$$F(x, s) = \frac{3\alpha}{\pi} \ln \frac{s}{m_e^2} \frac{1}{1-x} , \quad (14)$$

where  $\alpha$  is the electromagnetic coupling strength,  $m_e$  is the mass of the electron and  $x = \hat{s}/s$  is the squared centre of mass energy fraction of the event. (The

---

<sup>3</sup> In reality it resembles more a saddle than a box [14].

expression (14) can be derived, *e.g.*, from the  $e^-e^- \rightarrow L^{--}\gamma$  cross section (20), by singling out the large logarithm in the limit where  $m_B^2 \ll s$ .) Upon smearing the cross section (10) with the spectrum (14), we have

$$\begin{aligned} \sigma &= \int_0^1 dx F(x, s) \sigma(xs) \\ &\simeq \frac{S}{G} 2\alpha\lambda^2 \ln \frac{s}{m_e^2} \frac{1}{s - m_B^2} \quad (\Gamma_B \ll m_B \ll \sqrt{s}) . \end{aligned} \quad (15)$$

To estimate the discovery potential, we use the following scaling relation for the  $e^-e^-$  luminosity

$$\mathcal{L}_{e^-e^-} = 3.25 \cdot 10^7 s \quad , \quad (16)$$

which closely corresponds to a luminosity of  $25 \text{ fb}^{-1}$  at  $\sqrt{s} = 500 \text{ GeV}$  which scales like the square of the centre of mass energy. This choice for the luminosity is dictated by the latest  $e^+e^-$  linear collider design reports [14] and the fact that the  $e^-e^-$  mode will approximately suffer a 50% luminosity reduction because of the anti-pinch effect [16].

If we assume that observing one flavour violating  $e^-e^- \rightarrow \mu^-\mu^-$  event already constitutes a discovery, we need an average number of  $-\ln(1-p)$  Poisson distributed events such that *at least* 1 event is observed with probability  $p$ . Hence, a predicted average of at least 3 events is needed to guarantee a discovery with 95% confidence.

These considerations imply that the minimal value of the lepton-bilepton coupling  $\lambda$  needed to observe at least one  $e^-e^- \rightarrow \mu^-\mu^-$  event at the 95% confidence level on the resonance is according to Eqs (12,13)

$$\lambda \gtrsim 10^{-4} \sqrt{\frac{G}{S} \frac{6}{25\pi}} \simeq \frac{1}{4} 10^{-4} \sqrt{\frac{G}{S}} . \quad (17)$$

Similarly, according to the cross section (15), far off the resonance the minimal coupling is

$$\lambda \gtrsim 10^{-4} \sqrt{\frac{G}{S} \frac{4}{\alpha \ln \frac{s}{m_e^2}} \frac{s - m_B^2}{s}} \simeq \frac{1}{2} 10^{-3} \sqrt{\frac{G}{S}} . \quad (18)$$

Of course, the initial state radiation spectrum (14) is only an approximation, which at least has the virtue of yielding qualitative analytic results. We now

present the results of a more precise numerical convolution with a more realistic resummed luminosity distribution [17]. We also assume a polarization of 90% for the incoming electron beams.

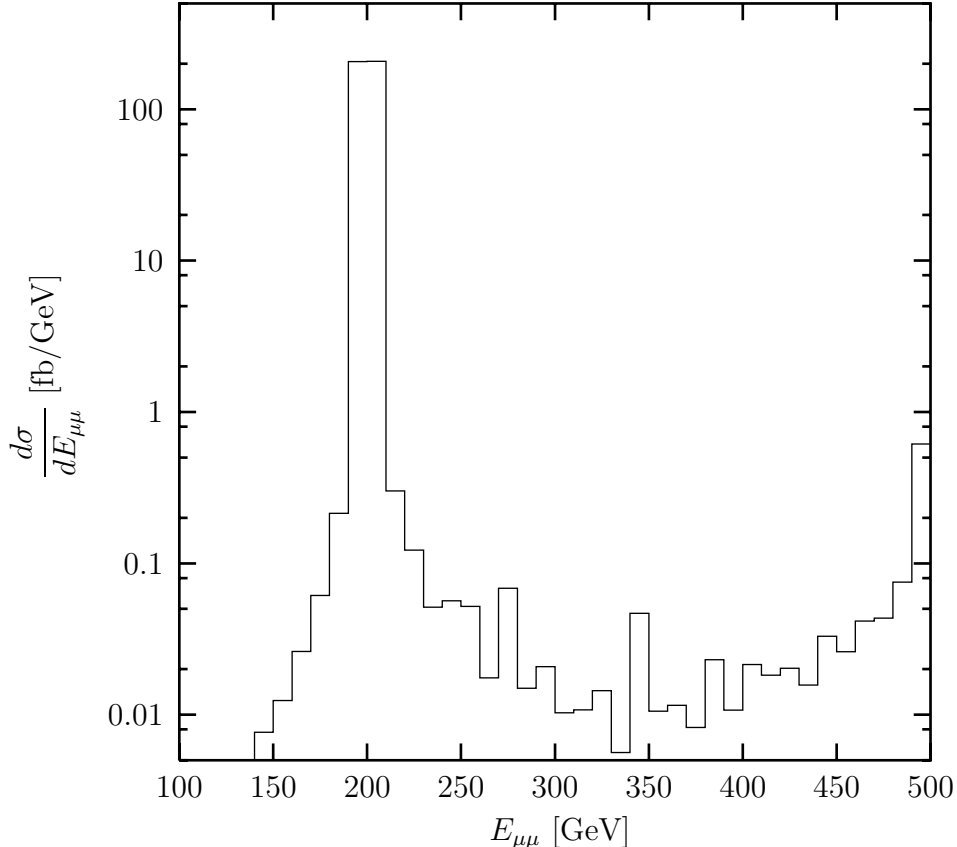


Fig. 2. Energy distribution of the muon pairs in the reaction  $e^-e^- \rightarrow \mu^-\mu^-$  at the centre of mass energy  $\sqrt{s} = 500$  GeV. This process is mediated by a doubly-charged vector bilepton  $L_{2\mu}^{--}$  of mass  $m_B = 200$  GeV which couples with strength  $\lambda = 0.1$  to the leptons (2). The peak at  $E_{\mu\mu} = m_B = 200$  GeV results from the radiative return to the bilepton resonance due to initial state radiation.

In Fig. 2 we show the energy distribution of the muon pairs over its full range. The peak at 200 GeV corresponds to the mass of a vector bilepton  $L_{2\mu}^{--}$  exchanged in the  $s$ -channel. The coupling to leptons is set to  $\lambda = 0.1$ . Fig. 3 displays a zoom into this peak region for different values of the coupling. The effect of the radiative return to the resonance is important even for bilepton masses far below the nominal collider energy. This suggests that no painstaking energy scan may be needed to localize a possible narrow bilepton resonance.

In Fig. 4 we show for several typical centre of mass energies the curves in the  $(m_B, \lambda)$  parameter space which correspond to having a 95% probability of



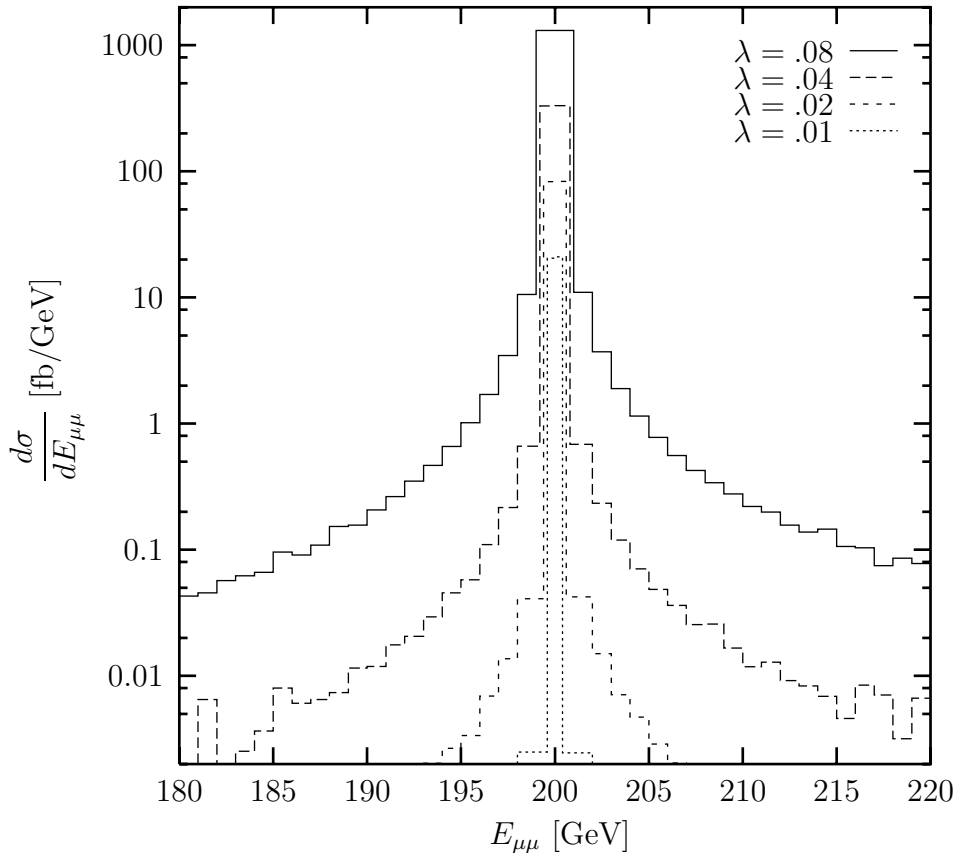


Fig. 3. Same as Fig. 2 for different values of the lepton-bilepton coupling  $\lambda$  and focusing on the muon energy region located around the peak. For the purpose of a clear display the two centremost bins for smaller couplings are depicted narrower than in the simulation. Their actual size is 1 GeV, like all other bins.

seeing a  $e^-e^- \rightarrow \mu^-\mu^-$  event due to the  $s$ -channel exchange of a vector bilepton  $L_{2\mu}^{--}$ . As expected the sensitivity is maximal when  $m_B = \sqrt{s}$  and worsens dramatically below threshold. Beyond threshold, however, the sensitivity is at worst decreased by about an order magnitude.

These results turn out to be actually quite close to the analytical predictions of Eqs (17,18). As expected according to these relations, the corresponding limits for the singlet  $\tilde{L}_1^{--}$  and triplet  $L_3^{--}$  bileptons are shifted down by factors of  $\sqrt{2}$  and 2, respectively.

While we have chosen the bilepton-lepton coupling matrix to be of the form (2), off-diagonal matrix elements  $\lambda^{ij}$  ( $i \neq j$ ) are in principle also allowed. For instance, in the case of scalar bileptons  $\lambda^{ij}$  is a matrix of Yukawa couplings which, in general, need not be flavour diagonal and would lead to different final states in the processes  $e^-e^- \rightarrow \ell_i^-\ell_j^-$ . In the presence of such non-diagonal

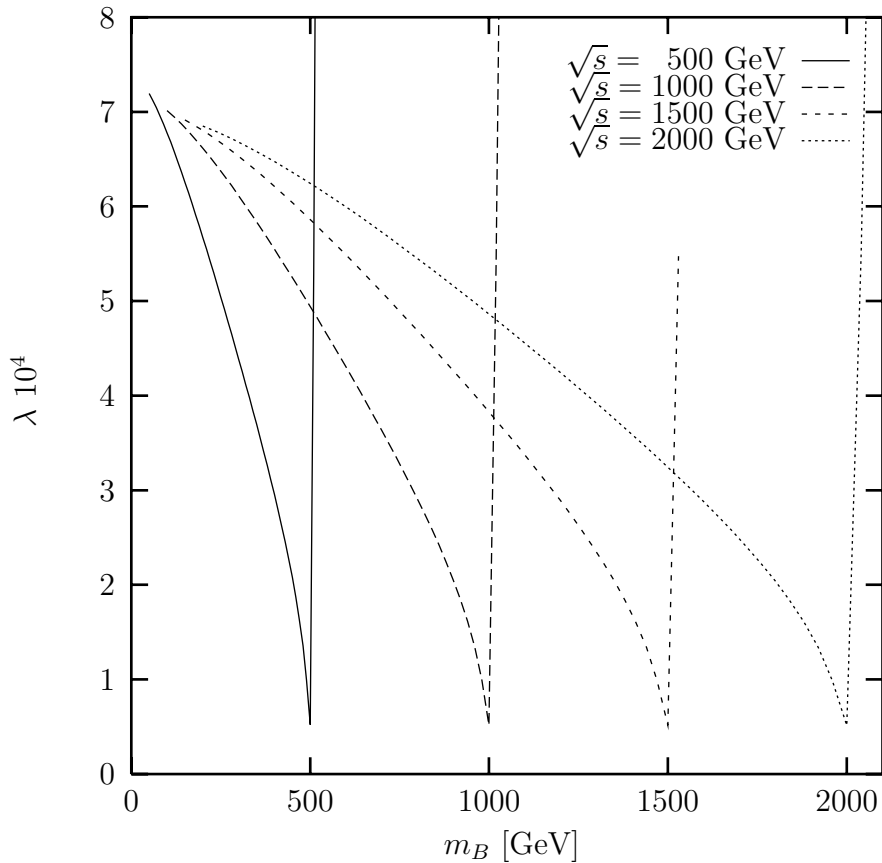


Fig. 4. Discovery prospects of a doubly-charged vector bilepton  $L_{2\mu}^{--}$  as a function of its mass  $m_B$  and coupling to leptons  $\lambda$  (2) for several values of the cm energy  $\sqrt{s}$ . In the absence of any  $e^-e^- \rightarrow \mu^-\mu^-$  event, the areas below and to the right of the curves cannot be excluded to better than 95% confidence.

couplings the quantity plotted in Fig. 4 against bilepton mass  $m_B$  becomes  $\lambda^{ee} \lambda^{ij} / \sqrt{\sum_{kl} (\lambda^{kl})^2} / 3$ . It could thus be that the electron-bilepton coupling  $\lambda^{ee}$  is too small (much less than  $10^{-4}$ ) to preclude the discovery of bileptons in  $e^-e^-$  collisions. In this case they can still be pair- or singly-produced at a linear collider in  $e^+e^-$ ,  $\gamma\gamma$  and  $e^-\gamma$  scattering [18].

The low-energy constraints on the off-diagonal couplings [8,19] are generally more stringent than the bound (3). Still, the combination of all linear collider operating modes will eventually probe the bileptons to exceedingly better sensitivities than any of the current experiments.

## 4 Determining the Nature of Bileptons

A standard way of determining the spin of a particle is to examine the angular distribution of its decay products. Obviously, scalar decays must be isotropic whereas vector decays will display some non-trivial angular dependence. This is clearly verified by the differential cross sections (6–8).

However, since the availability of high electron beam polarizations (in excess of 80%) is not a matter of debate [14], the polarization dependence of the scalar and vector total cross sections (10) will permit a much more straightforward determination of the spin of any discovered bilepton. Indeed, by flipping the helicity of one of the beams from the configuration with, say, two identical polarizations ( $P_1 = P_2 = P$ ) to the one with two opposite polarizations, ( $P_1 = -P_2 = P$ ) a scalar signal would be suppressed by a factor  $(1 - P^2)/(1 + P^2)^2$ , whereas a vector signal would be enhanced by a factor  $(1 + P^2)/(1 - P^2)$ . Even with a polarization of only 80% ( $P = 0.8$ ), this would mean a reduction or increase of the signal by respectively factors of almost 10 and 5. There is no way such a dramatic effect would escape detection.

However, determining the gauge nature of a discovered doubly-charged vector bilepton  $L_{2\mu}^{--}$  is not such an easy task. It will necessarily involve a precise study of the interaction between photons and bileptons, according to Eq. (4).

We propose here a method based on the reaction

$$e^-e^- \rightarrow L_{2\mu}^{--}\gamma, \quad (19)$$

which proceeds through the three Feynman diagrams depicted in Fig. 5. The third of these graphs involves the bilepton-photon coupling. As before, the lepton-flavour-violating decays of the produced bilepton guarantee an unmistakable background-free signal.

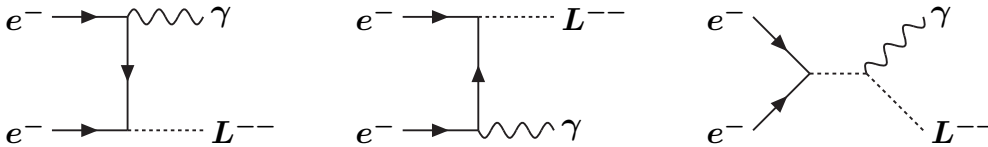


Fig. 5. Lowest order Feynman diagrams responsible for the reaction  $e^-e^- \rightarrow L_{2\mu}^{--}\gamma$ .

The total cross section of the process (19) is given by

$$\begin{aligned}
\sigma = \frac{\alpha\lambda^2}{3(s - m_B^2)} & \left\{ \frac{1 + P^2}{2} 3\Lambda^2 \right. & (20) \\
& + \frac{1 - P^2}{2} \left[ -\kappa^2 (1 + \Lambda - \Lambda^2) \right. \\
& \quad + 2\kappa (1 + \Lambda - 2\Lambda^2) \\
& \quad - 37 + 35\Lambda - 17\Lambda^2 \\
& \quad + 6(\Lambda^2 - 2\Lambda + 2) \ln \frac{1 + \rho}{1 - \rho} \\
& \quad \left. \left. + \frac{s}{m_B^2} (1 - \kappa)^2 \right] \right\} ,
\end{aligned}$$

where

$$\Lambda = 1 - \frac{m_B^2}{s} \quad \text{and} \quad \rho = \sqrt{1 - \frac{4m_e^2}{s}} . \quad (21)$$

Although we have set the electron mass  $m_e$  to zero wherever it is irrelevant in the final cross section (20), it is important to keep it finite throughout the calculation in order not to miss those terms which result from a cancellation of the electron mass in the numerator and the denominator. In particular, the *helicity flip* term on the first line is due to such a cancellation. As expected for such *helicity flip* terms, it vanishes at threshold where the photon energy is small.

Close to threshold the cross section (20) is dominated by the large logarithm in the penultimate term. Since this logarithm is solely due to the  $t$ - and  $u$ -channel electron exchanges, the gauge nature of the bilepton can only be revealed at higher energies. Away from threshold the last term, proportional to  $s/m_B^2$ , becomes increasingly more important. All the other terms are numerically irrelevant at all energies.

At asymptotic energies the cross section (20) saturates in the case of an ordinary vector with  $\kappa = 0$ . In contrast, if the produced bilepton is a Yang-Mills field with  $\kappa = 1$ , the cross section decreases like  $1/s$ . Although in principle this phenomenon may be used to distinguish these two cases, the onset of this asymptotic regime may be too slow to provide a useful test at the initial operating energies of the linear collider. This is demonstrated in Fig. 6, where we have plotted the energy dependence of the cross section (20) for an ordinary ( $\kappa = 0$ ) and a Yang-Mills ( $\kappa = 1$ ) bilepton of 200 GeV coupling with strength  $\lambda = 0.1$  to leptons. The difference is even smaller for heavier bileptons.

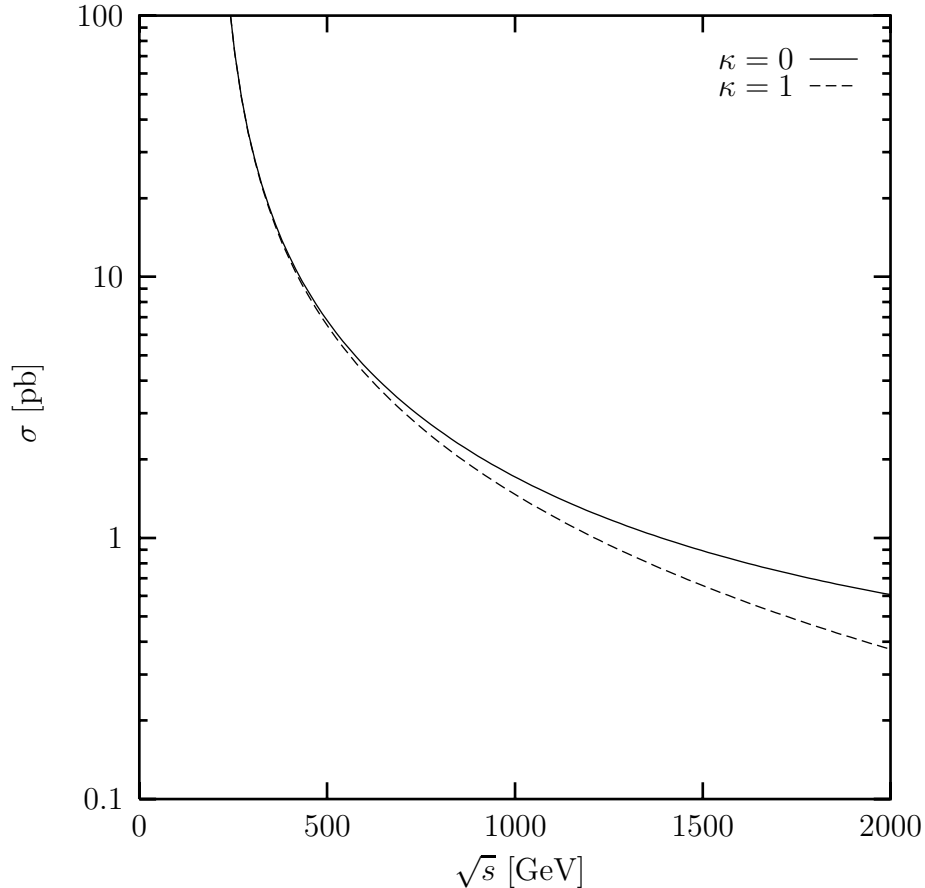


Fig. 6. Cross section for the process  $e^-e^- \rightarrow L_{2\mu}^- \gamma$  as a function of the centre of mass energy. The mass of the produced bilepton is 200 GeV and its coupling to leptons is 0.1.

However, the gauge nature of the bileptons may also be determined from the angular distribution of the emitted photons. We do not give here the analytical form of the differential cross section corresponding to the process (19), since it is long and not particularly enlightening. However, we plot this distribution in Fig. 7 for an ordinary and a Yang-Mills vector bilepton of mass 200 GeV at a centre of mass energy of 500 GeV. The most salient feature is the existence of an radiation amplitude zero in the transverse direction for the gauge bilepton.

To make efficient use of this difference in the angular distributions we perform a Kolmogorov-Smirnov test [20]. For this we first rewrite the angular distributions in term of the angular variable  $y = \cos^2 \theta$  in order to make advantageously use of the forward-backward symmetry of this process. We then integrate these new distributions from  $y = 0$  up to an arbitrary value of  $y$  such that  $y \leq \cos^2 \theta_{\min}$ , where  $\theta_{\min}$  is the smallest acceptance of the detector. This defines two cumulative probabilities (for  $\kappa = 0$  and  $\kappa = 1$ ) which increase

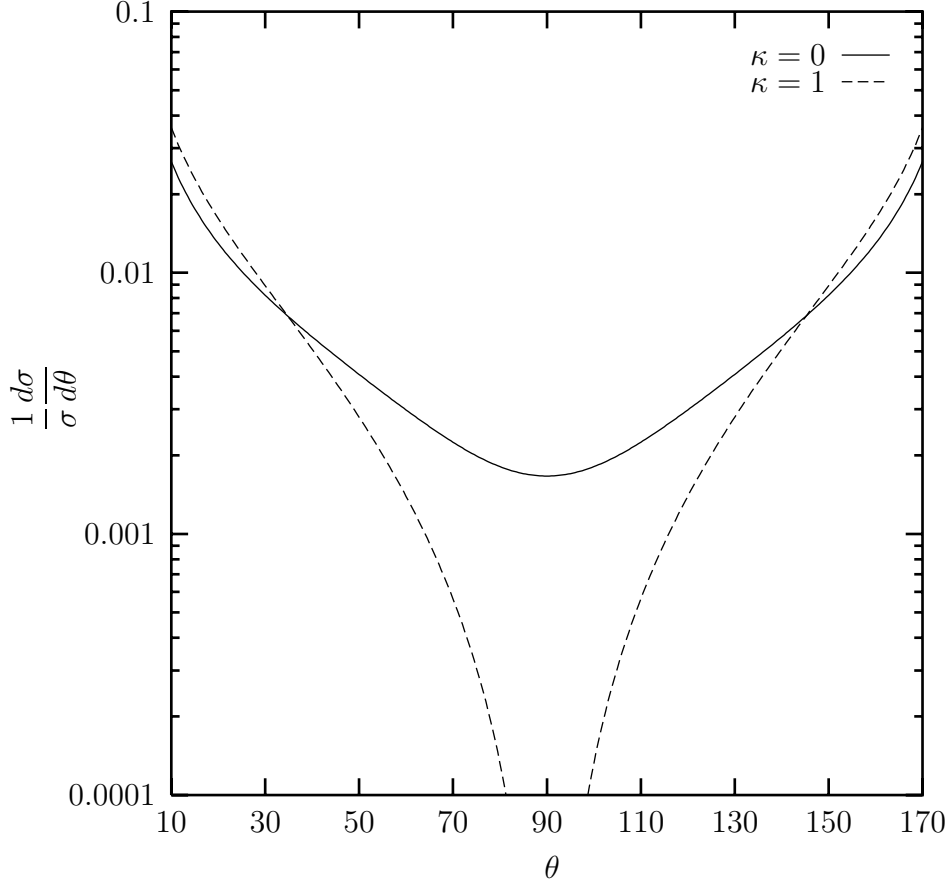


Fig. 7. Angular distribution of the process  $e^- e^- \rightarrow L_{2\mu}^- \gamma$  for a bilepton of 200 GeV and a centre of mass energy of 500 GeV.

monotonously as a function of  $y$  from 0 at  $y_{\min} = 0$  up to 1 at  $y_{\max} = \cos^2 \theta_{\min}$ . Between these boundaries the cumulative probabilities for the two cases are different. Somewhere in the middle of the range the difference between the cumulative probabilities is maximum. The Kolmogorov-Smirnov statistic  $D$  is defined as the product of this number times the square root of the number of observed events.

If we are dealing with, say, a Yang-Mills bilepton ( $\kappa = 1$ ), this cumulative probability is measured experimentally whereas the corresponding cumulative probability for the ordinary vector bilepton ( $\kappa = 0$ ) is computed. The Kolmogorov-Smirnov statistic is then given by

$$D = \sqrt{\mathcal{L} \int_0^{y_{\max}} dy \frac{d\sigma_1}{dy}} \max_y \left| \frac{\int_0^y dy \frac{d\sigma_1}{dy}}{\int_0^{y_{\max}} dy \frac{d\sigma_1}{dy}} - \frac{\int_0^y dy \frac{d\sigma_0}{dy}}{\int_0^{y_{\max}} dy \frac{d\sigma_0}{dy}} \right|, \quad (22)$$

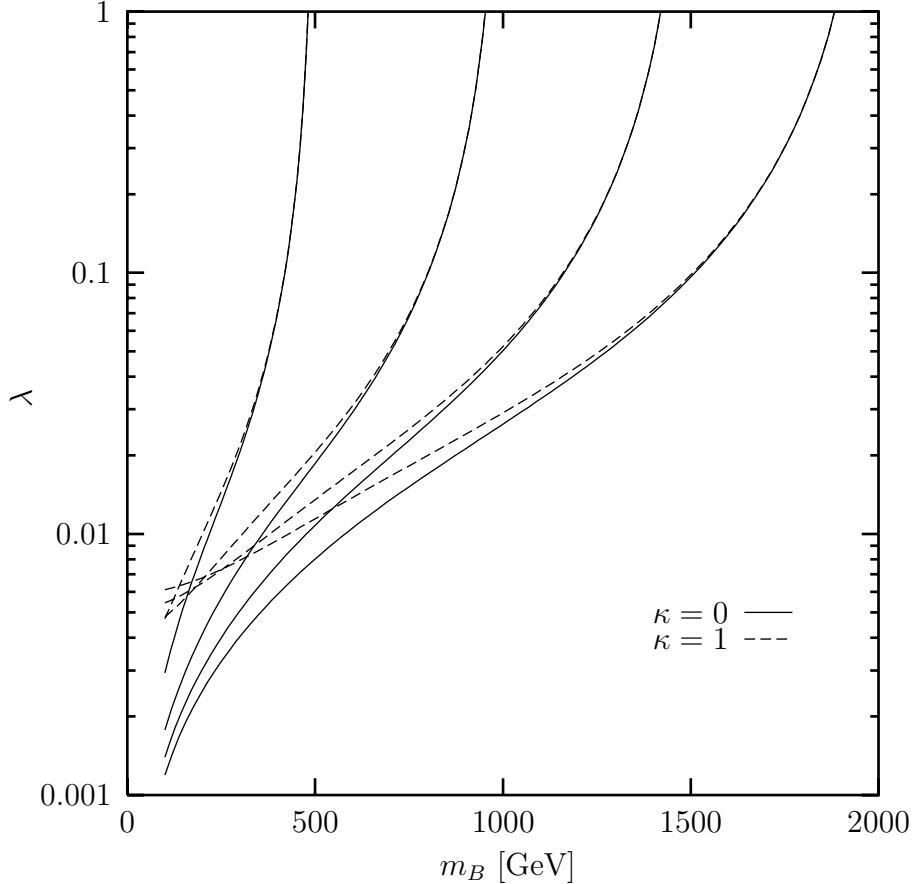


Fig. 8. Prospects for determining the gauge nature of a doubly-charged vector bilepton  $L_{2\mu}^{--}$  as a function of its mass  $m_B$  and coupling to leptons  $\lambda$  (2). The centre of mass energy increases from left to right as  $\sqrt{s} = 0.5, 1, 1.5$  and  $2$  TeV. The areas below and to the right of the curves do not allow a distinction between an ordinary vector and a Yang-Mills field to better than 99.9% confidence. The plain curves correspond to the case where the observed bilepton is an ordinary vector ( $\kappa = 0$ ) whereas the dashed curved correspond to the case where the observed bilepton is a Yang-Mills field ( $\kappa = 1$ ).

where the luminosity  $\mathcal{L}$  is given by Eq. (16) and the indices 0 and 1 refer to the cases  $\kappa = 0$  and  $\kappa = 1$ , respectively. If  $D = 1.95$  the observed  $\kappa = 1$  distribution has a probability of 99.9% to be different from a distribution which would have been observed if  $\kappa = 0$ . Of course, if the observed bilepton is an ordinary vector, the corresponding Kolmogorov-Smirnov statistic is obtained from Eq. (22) by interchanging the indices 0 and 1.

We have plotted in Fig. 8 the  $D = 1.95$  boundaries in the  $(m_B, \lambda)$  plane for different values of the centre of mass energy. The sensitivity increases the further away the bileptons are tested from threshold. Far from threshold the sensitivity is slightly better if the observed bileptons are ordinary vectors

rather than gauge bileptons, because of the larger event rates. In this case the distinction between the two types of bileptons can be made for values of the coupling  $\lambda$  as low as a few per mil.

## 5 Conclusions

We have investigated the potential of the  $e^-e^-$  collision mode of a linear collider for discovering and studying doubly-charged bileptons in a model-independent way. For this we have used the most general renormalizable lepton-bilepton and photon-bilepton interactions for scalar and vector bileptons belonging to different representations of the  $SU(2)_L$  gauge group, and we have studied the  $s$ -channel process  $e^-e^- \rightarrow \mu^-\mu^-$  taking into account the effects of initial state radiation, beam spread and polarization.

As expected, the linear collider sensitivity to bilepton properties is best when running on the resonance  $\sqrt{s} = m_B$ . With the planned machine parameters couplings to fermions can be tested down to less than  $10^{-4}$  at the resonance. Far from the resonance there is still an important radiative return to the bilepton resonance due to initial state radiation, which makes it possible to discover bileptons for couplings down to less than  $10^{-3}$  without having to resort to a collider energy scan.

If a bilepton is discovered, its nature can be investigated with several methods. The simplest way to discriminate between scalar and vector bileptons is to make use of polarization, since flipping the helicity of the incoming electron beams would increase or decrease the production cross sections differently. The knowledge of its spin is thus a free by-product of the discovery of a bilepton.

Recognizing Yang-Mills bileptons from minimally coupled vectors can be done by detecting hard photons in the process  $e^-e^- \rightarrow L_{2\mu}^-\gamma$ . Because the angular distributions are different the gauge nature of a light bilepton can easily be tested for couplings as small as  $10^{-2}$  or even smaller.

## Acknowledgments

We are thankful to Dirk Graudenz for his careful reading of the manuscript. M.R. thanks the Spanish Ministry of Education for a post-doctoral grant. His work is supported by the CICYT under grant AEN-96-1718.



## References

- [1] On-line information about the existing linear collider projects can be found on the following URLs  
CLIC: <http://www.cern.ch/CERN/Divisions/PS/CLIC/Welcome.html>  
JLC: <http://jlcux1.kek.jp/index-e.html>  
NLC: <http://nlc.physics.upenn.edu/nlc/nlc.html>  
TESLA: <http://www-tesla.desy.de:8080/>.
- [2] A comprehensive bibliography of high energy  $e^-e^-$  scattering can be found in <http://www.hep.psi.ch/e-e-.html>.
- [3] P.H. Frampton, B.H. Lee, *Phys. Rev. Lett.* **64** (1990) 619;  
P.B. Pal, *Phys. Rev.* **D 43** (1991) 236;  
P. Frampton *Phys. Rev. Lett.* **69** (1992) 2889;  
F. Pisano, V. Pleitez *Phys. Rev.* **D46** (1992) 410 [hep-ph/9206242];  
P. Frampton, *Mod. Phys. Lett.* **A7**, (1992) 2017.
- [4] H. Georgi, M. Machacek, *Nucl. Phys.* **B 262** (1985) 463;  
K.S. Babu, V.S. Mathur, *Phys. Lett.* **B 196** (1987) 218;  
J.C. Pati, A. Salam, *Phys. Rev.* **D10** (1974) 275;  
R.N. Mohapatra, J.C. Pati, *Phys. Rev.* **D11** (1975) 566, *ibid.* 2558;  
G. Senjanovic, R.N. Mohapatra, *Phys. Rev.* **D 12** (1975) 1502;  
R.N. Mohapatra, G. Senjanovic, *Phys. Rev.* **D 23** (1981) 165.
- [5] G.G. Ross “Grand Unified Theories”, (1985) Benjamin-Cummins, Menlo Park;  
E. Fahri, L. Susskind, *Phys. Rep.* **74** (1981) 277;  
E. Eichten et al., *Rev. Mod. Phys.* **56** (1984) 579.
- [6] W. Buchmüller, *Acta Phys. Austr. Suppl XXVII* (1985) 517;  
B. Schrempp, Proc. of the XXIII Int. Conf. on High Energy Physics Berkeley.
- [7] T.P. Cheng, L. Li, *Phys. Rev.* **D 22** (1980) 2860;  
G.B. Gelmini, M. Roncadelli, *Phys. Lett.* **B 99** (1981) 411;  
A. Zee, *Phys. Lett.* **B 93** (1980) 389;  
R. Peccei, *The Physics of Neutrinos*, Proc. of the Flavour Symposium, Peking University, August 1988.
- [8] F. Cuypers, S. Davidson, MPI & PSI preprints MPI-PhT/96-45, PSI-PR-96-21 [hep-ph/9609487].
- [9] W. Buchmüller, R. Rückl, D. Wyler, *Phys. Lett.* **B191** (1987) 442.
- [10] T. Rizzo, *Phys. Rev.* **D 25** (1982) 1355;  
T. Rizzo, *Phys. Rev.* **D 46** (1992) 910;  
P. Frampton, D. Ng, *Phys. Rev.* **D 45** (1992) 4240;  
J. Maalampi, A. Pietilä, M. Raidal, *Phys. Rev.* **D 48** (1993) 4467.
- [11] J.F. Gunion, *Int. J. Mod. Phys.* **A11** (1996) 1551.

- [12] W. Bertl, Proceedings of the Workshop *Weak & Electromagnetic Interactions in Nuclei*, Osaka, June 1995, Eds: H. Ejiri, T. Kishimoto, T. Sato; R. Abela *et al.*, *Phys. Rev. Lett.* **77** (1996) 1950.
- [13] M.D. Swartz, *Phys. Rev.* **D 40** (1989) 1521;  
 J.A. Grifols, A. Mendez, G.A. Schuler, *Mod. Phys. Lett.* **A 4** (1989) 1485;  
 J.F. Gunion, J.A. Grifols, A. Mendez, B. Kayser, F. Olness, *Phys. Rev.* **D 40** (1989) 1546.
- [14] NLC Design Group, *Zeroth-Order Design Report for the Next Linear Collider*, Vol. 2, SLAC-R-0474-VOL-2 [<http://www.slac.stanford.edu/accel/nlc/zdr>].
- [15] The  $\mu^+\mu^-$  Collider Collaboration, *Muon Muon Collider: Feasibility Study*, BNL-52503.
- [16] J.E. Spencer, *Int. J. Mod. Phys.* **A11** (1996) 1675.
- [17] É.A. Kuraev, V.S. Fadin, *Sov. J. Nucl. Phys.* **41** (1985) 466.
- [18] See, for example:  
 N. Lepore, B. Thorndyke, H. Nadeau, D. London, *Phys. Rev.* **D 50** (1994) 2031;  
 G. Barenboim, K. Huitu, J. Maalampi, M. Raidal, *Phys. Lett.* **B 394** (1997) 132 [[hep-ph/9611362](http://arxiv.org/abs/hep-ph/9611362)],  
 and references therein.
- [19] R. Mohapatra, *Phys. Rev.* **D 46** (1992) 2990.
- [20] W.T. Eadie *et al.*, *Statistical Methods in Experimental Physics*, North Holland, 1971.